文章编号：1000-5773(2009)04-0288-11

Analytic Equation of State for Generalized Morse Potential Fluid and Application to N_2 Fluid*

XUE Xin-Ying, SUN Jiu-Xun, TIAN Rong-Gang

(*Department of Applied Physics, University of Electronic Science and Technology, Chengdu* 610054, *China*)

Abstract: The analytic expressions for equation of state (EOS) and thermodynamic properties have been derived for the generalized Morse (GM) potential fluids, by using the Ross variational perturbation theory and the analytic Percus-Yevick (PY) expression of radial distribution function of hard spheres. Extensive comparison of the numerical results with computer simulations shows that the precision of the analytic Ross theory is equivalent to or slightly better than the non-analytic modified Weeks-Chandler-Anderson (mWCA) theory, and is much better than the complicated optimized reference hyper-netted chain (RHNC) theory. This analytic expressions for equation of state have been applied to N_2 fluid at ambient temperature and low pressure (below 1 GPa) with the parameters of the generalized Morse potential are obtained by fitting to experimental data, results of prediction of the pressure above 1 GPa validate the analytic EOS with good agreement within a wide range of pressure and temperature.

Key words: equation of state; thermodynamic quantities; analyticity; variational

CLC number: O521.2 **Document code**: A

1 Introduction

The perturbation theories such as the Barker-Henderson[1], the Weeks-Chandler-Anderson (WCA)[2] and the Ross theories[3] are most frequently used in research of thermodynamic properties for fluids both at normal condition and at the condition with high temperature and high density. The Ross theory, among the most accurate perturbation theories, has been widely used to the research of shock-compressed properties of materials[4-5]. Its main disadvantage lies in the variational procedure being time-consuming and inconvenient in the shock-compressing and melting problems calculations. In order to overcome these shortcomings, Tang et al. have alternatively developed a mean spherical approximation (MSA) theory[6-8]. However, the MSA theory itself has some disadvantages even severer than the Ross theory. The most important one is that the MSA theory is inapplicable to the fluids with high temperature and density, and at other conditions the theory gives results comparable with the Ross theory or even poorer.

Kang et al.[9] have modified the WCA (mWCA) theory applicable to the fluids at high tempera-

* **Received date**: 2008-10-16; **Revised date**: 2009-03-16

Foundation item: The Joint Fund of NSFC and CAEP(10476007); by the Support Programs for Academic Excellence of the Education Ministry of China(NCET-05-0799); UESTC(23601008)

Biography: XUE Xin-Ying(1970—), male, doctor of physics. Main Instrest: Equation of state of the simple fluids. E-mail: yyingxx@163.com

Corresponding author: SUN Jiu-Xun (1967—), male, doctor of physics, professor. Main Instrest: Equation of state of the fluids and solids, phase equilibrium and phase transition. E-mail: sjx@uestc.edu.cn

ture and pressure condition without the introduction of variational procedure. And Lado et al.[10-11] also proposed an optimized reference hyper-netted chain (RHNC) theory. Talbot et al.[12] tested the Ross, mWCA and RHNC theories for predicting the equilibrium properties of spherical fluids with conclusion that the Ross and mWCA theories give very good results for the thermodynamic properties, but not for the structure, while the RHNC theory requires more computer time but yields satisfactory results both for thermodynamic properties and structure. If one's interest is restricted to the thermodynamic properties, then it is sufficient to use the Ross or mWCA theories, and no need for computer simulations of classical systems of particles interacting with spherical potentials. Recently, Vortler et al.[13] also tested the mWCA and RHNC for the Exp-6 fluids within wider temperature and pressure ranges. Their conclusion is in accordance with that of Talbot et al.[12].

If the Ross theory can provide an analytic equation of state (EOS), it may have more advantages than many other invariational perturbation theories. Due to little attention paid to the interaction with the generalized Morse (GM) fluid, it is important to develop an analytic EOS for the GM potential. In this paper we will show that the analytic expressions for EOS and thermodynamic properties for the generalized Morse potential can be directly derived based on the Ross theory and the Percus-Yevick (PY) HS-RDF[14-15]. There is no need of other approximations, and the applicability of the analytic formalism is as same as the original non-analytic Ross theory. On account of the absence of the data available for GM potential fluid, the form of which is determined by fitting Exp-6 potential with least square method and the parameters of which are obtained by fitting experimental data for Exp-6 potential fluids.

Nitrogen has been one of the most important reference fluids both for test of physical models and for calibration purposes, the investigation of which is of great importance and draw considerable interest especially at high pressure region. Knowledge of the equation of state for dense nitrogen is of importance for technologies as well as for the general understanding of the behavior of matter at extreme condition. Various models and theories have been used to study the behavior of nitrogen at very high pressure with abundant experimental data and simulation results[16-21]. It is practically meaningful to examine the application of the new EOS to N_2 fluid in a wide range of pressure and temperature.

The paper is organized as follows: In section Ⅱ, the main formalism of Ross theory is outlined. And the analytic expressions of EOS and thermodynamic properties of GM fluids are developed. In section Ⅲ, the fitting results of GM potential to Exp-6 potential are presented. In section Ⅳ, the validity of new EOS is demonstrated by compare with the MD simulations, non-analytic mWCA and RHNC theories. In section Ⅴ, the new EOS is applied to N_2 fluid with further intention to examine the applicability to real fluids. The summary is presented in section Ⅵ.

2 Theory

In terms of the Ross perturbation theory[3], the Helmholtz free energy is expressed as follows

$$\frac{F}{NkT}=\frac{F_0}{NkT}+\frac{F_1}{NkT}+\frac{F_{12}(\eta)}{NkT} \tag{1}$$

where F_0 is the free energy of reference hard-sphere system[22], and

$$\frac{F_1}{NkT}=2\pi\rho\beta\int_d^\infty \varphi(r)g(r)r^2\,\mathrm{d}r \tag{2}$$

is the first-order perturbation. $\varphi(r)$ is the potential function, $g(r)$ is the HS-RDF. $F_{12}(\eta)$ is a function making Eq. (1) reproduce the MC inverse 12th-power results[3]

$$\frac{F_{12}(\eta)}{NkT}=-\left(\frac{\eta}{2}+\eta^2+\frac{\eta^4}{2}\right) \tag{3}$$

where $\eta=\pi\rho d^3/6$, d is the hard sphere diameter, and η is employed as the variational parameter that minimizes the right side of Eq. (1). Namely, η should be determined by

$$\frac{\partial}{\partial\eta}\left(\frac{F}{NkT}\right)_{T,\rho}=\frac{\partial}{\partial\eta}\left(\frac{F}{NkT}\right)_{T,\eta_e}=0 \tag{4}$$

The integral in Eq. (2) can be transformed to following form[23]

$$\frac{F_1}{NkT}=12\eta\beta\int_1^\infty\varphi(x)g(x)x^2\mathrm{d}x=12\eta\beta\int_0^\infty\Phi(t)G(t)\mathrm{d}t \tag{5}$$

Where $x=r/d$ is the radial coordination reduced to the hard sphere diameter and $\Phi(t)$ is the inverse Laplace transformation of $x\varphi(x)$

$$\Phi(t)=L^{-1}[x\varphi(x)] \tag{6}$$

$G(t)$ is the Laplace transformation of $[rg(r)]$. The PY expression of $G(t)$ and derivatives with respect to η and t have been given in the appendix.

The GM potential has following form

$$\varphi(r)=\varepsilon_0\sum_{i=1}^{n}C_i\mathrm{e}^{\alpha_i(1-r/r_e)} \tag{7}$$

The parameter ε_0 determines the depth of the potential minimum which is located at r_e and α determines the softness of the repulsion. Note that the parameters of the GM potential are obtained in next section by fitting the Exp-6 potential in least square method due to absence of reference data. Introducing following notations

$$\lambda=r_e/d=(\eta_e/\eta)^{1/3},\quad \eta_e=\pi\rho r_e^3/6 \tag{8}$$

The potential function in Eq. (7) can be reformulated as

$$\varphi(r)=\varepsilon_0\sum_{i=1}^{n}C_i\mathrm{e}^{\alpha_i(1-x/\lambda)} \tag{9}$$

By the aid of the mathematical formula

$$L^{-1}[x\mathrm{e}^{-\lambda x}]=\delta'(t-\lambda) \tag{10}$$

The inverse Laplace transformation of $x\varphi(x)$ can be derived as

$$\Phi(t)=\varepsilon_0\sum_{i=1}^{n}C_i\mathrm{e}^{\alpha_i}\delta'(t-\alpha_i\lambda^{-1}) \tag{11}$$

Where $\delta(t)$ is the Dirac delta function, and the prime ' ' represents the first order derivative with respect to the variable t. Substitution of Eq. (11) into Eq. (5) yields

$$\frac{F_1}{NkT}=-12\eta\beta\varepsilon_0\sum_{i=1}^{n}C_i\mathrm{e}^{\alpha_i}G'_t(\alpha_i\lambda^{-1}) \tag{12}$$

The compressibility factor can be derived as follows

$$\frac{pV}{NkT}=1+\rho\frac{\partial}{\partial\rho}\left(\frac{F}{NkT}\right)_T=1+\eta_e\frac{\partial}{\partial\eta_e}\left(\frac{F}{NkT}\right)_T=$$
$$1+\eta_e\frac{\partial}{\partial\eta_e}\left(\frac{F}{NkT}\right)_{T,\eta}+\frac{\partial}{\partial\eta}\left(\frac{F}{NkT}\right)_{T,\eta_e}\cdot\eta_e\frac{\partial\eta}{\partial\eta_e}$$

Considering Eq. (4), the third term in the equation equals zero, we obtain

$$\frac{pV}{NkT}=1+\eta_e\frac{\partial}{\partial\eta_e}\left(\frac{F}{NkT}\right)_{T,\eta}=1+\eta_e\frac{\partial}{\partial\eta_e}\left(\frac{F_1}{NkT}\right)_{T,\eta} \tag{13}$$

With Substitution of Eq. (12) into Eq. (13) yields

$$\frac{pV}{NkT}=1+4\eta\beta\varepsilon_0\sum_{i=1}^{n}C_i\mathrm{e}^{\alpha_i}(\alpha_i\lambda^{-1})G''_{tt}(\alpha_i\lambda^{-1}) \tag{14}$$

The equation for the internal energy is

$$\frac{U}{NkT}=\beta\frac{\partial}{\partial\beta}\left(\frac{F}{NkT}\right)_{\rho}=\beta\frac{\partial}{\partial\beta}\left(\frac{F}{NkT}\right)_{\eta}+\frac{\partial}{\partial\eta}\left(\frac{F}{NkT}\right)_{T,\eta_e}\cdot\beta\frac{\partial\eta}{\partial\beta}$$

Considering Eq. (4), the second term in the equation equals zero, and the equation is changed as

$$\frac{U}{NkT}=\beta\frac{\partial}{\partial\beta}\left(\frac{F}{NkT}\right)_{\eta}=\beta\frac{\partial}{\partial\beta}\left(\frac{F_1}{NkT}\right)_{\eta}=\frac{F_1}{NkT}\tag{15}$$

With Substitution of Eqs. (3, 12) into Eq. (1), and Eq. (1) into Eq. (4), the equation to determine η can be derived as

$$\frac{4-2\eta}{(1-\eta)^3}-\left(\frac{1}{2}+2\eta+2\eta^3\right)+\frac{\partial}{\partial\eta}\frac{F_1}{NkT}=0\tag{16}$$

$$\frac{\partial}{\partial\eta}\frac{F_1}{NkT}=\frac{1}{\eta}\left[\frac{F_1}{NkT}-\frac{pV}{NkT}+1\right]-12\eta\beta\varepsilon_0\sum_{i=1}^{n}C_i e^{\alpha_i}G''_{\eta t}(\alpha_i\lambda^{-1})\tag{17}$$

Although Eq. (16) is a nonlinear algebraic equation, by using the Newtonian iteration approach, its solution is insensitive to the initial value and is absolutely convergent.

3　Fitting of GM Potential to Exp-6 Potential

As mentioned above, we first fit the GM potential $\varphi(r)$ to the Exp-6 potential $\varepsilon(r)$

$$\varepsilon(r)=\frac{\varepsilon_0}{\alpha-6}\left[6e^{\alpha(1-r/r_e)}-\alpha\left(\frac{r_e}{r}\right)^6\right]\tag{18}$$

in least square method, during which the best value of n is found to be integer 3 and the parameter α_1 to be α, best reproducing the Exp-6 potential, the same as those α given in the case of Exp-6 potential[13], which can be easily explained in that the repulsive part gain dominance over the other attractive parts. In terms of least square method, $\varphi(r_e)$ is required to be ε_0, the first and the second derivation of $\varphi(r)$ with respect to r at equilibrium distance r_e is required to be equal to those of $\varepsilon(r)$, which yields

$$\begin{cases}C_1+C_2+C_3=-1\\ \alpha_1C_1+\alpha_2C_2+\alpha_3C_3=0\\ \alpha_1^2C_1+\alpha_2^2C_2+\alpha_3^2C_3=r_e^2\varepsilon''(r_e)\end{cases}\tag{19}$$

In terms of Eq. (19), there are only three independent variable left, and we choose α_1, α_2 and α_3 as parameters to be obtained by fitting. The fitting, as shown in Fig. 1, is satisfactory in general. It should be pointed out that the fitting over whole range of distance r is unfeasible and the deviation from Exp-6 potential may be increase rapidly as distance r tends to zero or infinity. In principle, the best fitting lies in the vicinity of equilibrium distance r_e in terms of Eq. (19), but it can be seen from Fig. 1 that the fitting is good over wide range of distance r, which suggests that the

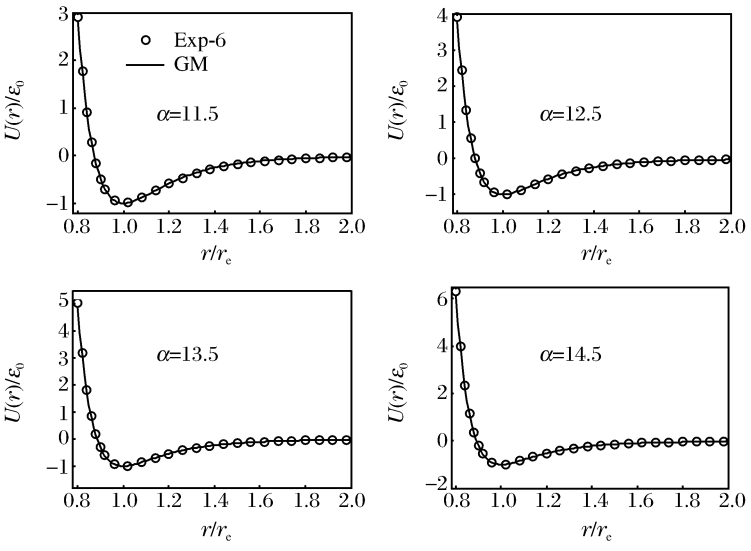


Fig. 1　The fitting results of generalized Morse potential to Exp-6 potential

fitting of GM potential to Exp-6 potential is resonable. The validity and applicability of the model will be examined in the next section by compare with simulation over wide range of density and temperature.

4 Demonstration of Validity

We compare the numerical results with the extensive simulations from the molecular dynamic (MD) simulations, mWCA and RHNC results from Vortler et al.[13]. Table 1～Table 4 present the comparison of the results of reduced pressure (pr_e^3/ε_0) and reduced internal energy ($U/N\varepsilon_0$) for the Exp-6 fluids with $\alpha = 11.5, 12.5, 13.5$ and 14.5, respectively, calculated in this work with those from

Table 1 Comparison of the results of reduced pressure(pr_e^3/ε_0) and reduced internal energy($U/N\varepsilon_0$) for the Exp-6 fluids with $\alpha=11.5$ calculated in this work(XS) with that of molecular dynamic simulations, mWCA and RHNC theories by Vortler et al.[13]

kT/ε_0	ρr_e^3	pr_e^3/ε_0				$U/N\varepsilon_0$			
		MD	Δ_{mWCA}	Δ_{RHNC}	Δ_{XS}	MD	Δ_{mWCA}	Δ_{RHNC}	Δ_{XS}
2	1.4	12.95	−0.27	−0.51	0.55	−5.33	−0.05	−0.12	−0.02
	1.6	24.73	−0.23	−0.75	0.53	−5.04	−0.04	−0.16	−0.02
	1.8	43.22	−0.56	−1.33	0.36	−4.18	−0.16	−0.36	0.06
	2.0	70.28	−0.96	−2.40	−0.04	−2.36	−0.14	−0.48	−0.02
	2.2	99.70	−9.68	−12.16	7.36	*−0.02	−0.56	−1.09	0.27
	2.3	121.7	−11.32	−14.50	8.14	*0.68	−1.62	−2.27	1.26
	2.4	152.6	−7.10	−11.43	11.69	3.40	−0.88	−1.72	1.11
3	1.6	32.45	−0.38	−0.82	0.91	−3.82	−0.05	−0.15	−0.01
	1.8	53.12	−0.50	−0.97	0.59	−2.58	−0.06	−0.19	−0.04
	2.0	82.13	−0.97	−1.80	0.39	*−0.69	−0.21	−0.44	0.06
	2.2	121.5	−1.85	−3.26	0.06	2.31	−0.21	−0.57	−0.05
	2.4	173.4	−2.78	−5.09	−0.80	6.30	−0.24	−0.79	−0.18
	2.6	232.4	−10.57	−14.63	4.98	*0.35	−11.29	−12.14	10.68
4	2.0	92.23	−1.21	−1.70	0.96	0.94	−0.10	−0.25	−0.06
	2.3	158.9	−2.28	−3.27	0.17	6.00	−0.20	0.53	−0.11
	2.4	187.4	−2.87	−4.09	−0.20	8.24	−0.23	−0.61	−0.19
	2.6	254.9	−4.06	−6.43	−0.90	13.40	−0.36	−0.96	−0.24
	2.9	364.7	−27.73	−32.73	18.95	21.60	−2.28	−3.33	1.31
6	2.3	181.4	−2.53	−2.60	1.27	9.09	−0.23	−0.41	−0.08
	2.5	244.8	−4.10	−4.19	1.09	14.1	−0.35	−0.59	−0.15
	2.7	323.6	−5.10	−5.72	0.18	20.10	−0.54	−0.93	−0.16
	3.0	473.0	−7.42	−9.24	−1.37	31.62	−0.54	−0.20	−0.60
	3.3	632.3	−41.89	−46.43	29.08	40.80	−5.52	−6.67	3.91
	3.6	882.6	−32.16	−41.28	15.00	59.58	−3.60	−5.49	1.51
8	2.4	232.4	−3.43	−2.92	2.30	14.24	−0.35	−0.45	−0.05
	2.9	446.8	−6.99	−6.52	1.18	30.80	−0.72	−1.06	−0.20
	3.2	627.6	−10.10	−10.09	0.37	44.16	−1.12	−1.61	−0.34
	3.5	854.2	−12.40	−15.03	−1.14	60.40	−1.20	−2.26	−0.73
	3.8	1085.8	−59.06	—	42.02	74.64	−6.16	—	3.59
15	2.4	294.4	−2.23	−2.88	4.78	22.35	−0.25	−0.52	−0.14
	3.2	722.0	−6.64	—	7.64	55.35	−1.20	—	−0.30
	3.6	1048.8	−16.62	—	10.92	78.75	−1.65	—	−0.52
	4.0	1466.0	−21.40	—	14.66	106.95	−2.10	—	−0.82
	4.4	1978.0	−29.06	—	23.99	139.95	−2.55	—	−1.17
Average errors/(%)			2.59	3.69	1.82		4.65	10.2	2.96

Note: (a) The parameters(α_2, α_3) in the generalized morse-potential used in the calculation are (5.22, 1.52) for $\alpha_1 = 11.5$.
(b) Numbers in columns labeled as Δ_{mWCA}, Δ_{RHNC} and Δ_{XS} denote the respective deviations from the simulation results, $\Delta_{(\cdots)} = X_{simul} - X_{(\cdots)}$. The data points labeled '*' have not been included in the calculations of errors.

MD simulations, mWCA and RHNC theories by Vortler et al.[13]. In Table 5, the calculated results of the analytic Ross theory are shown in good agreement with the MC simulations with much better results than that of the RHNC theory and slightly higher precision than that of mWCA theory, which verifies the reliability of the analytic Ross theory and validity of the model developed in this paper. Table 6 presents five sets of parameters (α_2, α_3) corresponding to the five cases of values of parameter α_1.

In general, the model of this work is reasonable and the results from Ross theory are preferable to those from mWCA and RHNC theory.

Table 2　Comparison of the results of reduced pressure(pr_e^3/ε_0) and reduced internal energy($U/N\varepsilon_0$) for the Exp-6 fluids with α=12.5 calculated in this work(XS) with that of molecular dynamic simulations, mWCA and RHNC theories by Vortler et al.[13]

kT/ε_0	ρr_e^3	pr_e^3/ε_0				$U/N\varepsilon_0$			
		MD	Δ_{mWCA}	Δ_{RHNC}	Δ_{XS}	MD	Δ_{mWCA}	Δ_{RHNC}	Δ_{XS}
2	1.5	21.71	−0.39	−1.02	0.37	−4.92	−0.04	−0.16	−0.25
	1.7	40.36	−0.37	−1.50	−0.14	−4.16	−0.10	−0.33	−0.22
	1.9	69.06	−0.63	−2.72	−0.99	−2.32	−0.06	−0.44	−0.39
	2.1	103.3	−8.34	−12.27	5.05	*0.04	−0.58	−1.27	0.01
3	1.6	39.06	−0.32	−0.97	0.25	−3.27	−0.02	−0.14	−0.29
	1.8	64.51	−0.78	−1.81	0.01	−1.86	−0.18	−0.40	−0.19
	2.0	101.9	−1.06	−3.06	−0.94	*0.75	−0.18	−0.57	−0.30
	2.2	146.0	−9.43	−13.05	5.37	3.90	−0.84	−1.50	0.20
	2.3	168.6	−19.53	−24.25	14.09	4.50	−2.65	−3.48	1.90
4	1.7	59.30	−0.55	−1.31	0.44	−1.38	−0.05	−0.20	−0.27
	1.9	92.61	−0.97	−2.04	−0.11	*0.93	−0.07	−0.30	−0.34
	2.1	139.1	−1.52	−3.49	−1.00	4.20	−0.24	−0.64	−0.30
	2.3	201.7	−2.45	−5.88	−2.69	8.92	−0.24	−0.91	−0.48
	2.5	269.0	−18.10	−23.68	9.30	13.80	−1.56	−2.56	0.54
6	1.9	111.9	−1.04	−1.70	0.22	3.54	−0.13	−0.25	−0.34
	2.1	162.5	−1.43	−2.62	−0.69	7.20	−0.30	−0.56	−0.24
	2.3	229.1	−2.60	−4.56	−1.88	12.30	−0.36	−0.79	−0.36
	2.6	366.2	−4.92	−8.97	−5.37	22.62	−0.54	−1.35	−0.65
8	2.1	182.8	−1.50	−2.30	−0.37	9.84	−0.24	−0.49	−0.25
	2.3	253.1	−2.70	−3.84	−1.33	15.44	−0.21	−0.54	−0.50
	2.4	295.1	−3.65	−5.12	−1.90	18.56	−0.40	−0.79	−0.44
	2.7	454.8	−6.36	−9.20	−5.90	30.48	−0.72	−1.40	−0.67
	3.0	634.6	−45.08	−52.23	24.22	41.60	−5.36	−6.73	3.39
15	2.3	323.3	−2.22	−9.18	−0.44	24.00	−0.23	−1.30	−0.52
	2.5	424.0	−3.50	—	−1.80	31.80	−0.45	—	−0.58
	2.8	618.4	−6.98	—	−5.42	46.35	−0.75	—	−0.78
	3.1	872.6	−11.83	—	−10.84	64.65	−1.20	—	−1.16
	3.4	1 197.1	−40.42	—	−19.81	87.15	−3.75	—	−1.96
	3.7	1 517.0	−103.60	—	51.02	106.35	−9.15	—	4.52
Average errors/(%)			2.55	4.15	1.57		6.65	14.1	6.95

Note: (a) The parameters(α_2, α_3) in the generalized morse-potential used in the calculation are (5.60, 1.74) for α_1=12.5.
(b) Numbers in columns labeled as Δ_{mWCA}, Δ_{RHNC} and Δ_{XS} denote the respective deviations from the simulation results, $\Delta_{(...)} = X_{simul} - X_{(...)}$. The data points labeled '*' have not been included in the calculations of errors.

Table 3 Comparison of the results of reduced pressure(pr_e^3/ε_0) and reduced internal energy($U/N\varepsilon_0$) for the Exp-6 fluids with $\alpha=13.5$ calculated in this work(XS) with that of molecular dynamic simulations, mWCA and RHNC theories by Vortler et al.[13]

kT/ε_0	ρr_e^3	pr_e^3/ε_0				$U/N\varepsilon_0$			
		MD	Δ_{mWCA}	Δ_{RHNC}	Δ_{XS}	MD	Δ_{mWCA}	Δ_{RHNC}	Δ_{XS}
2	1.0	4.176	0.10	−0.05	−0.11	−4.18	−0.06	−0.06	−0.06
	1.2	8.88	0.02	−0.22	0.08	−4.70	−0.02	−0.06	−0.09
	1.4	18.31	−0.03	−0.55	0.21	−4.80	0.00	−0.10	−0.10
	1.6	35.10	−0.23	−1.43	0.26	−4.32	−0.10	−0.31	−0.01
3	1.3	19.18	−0.12	−0.38	0.26	−4.02	−0.12	−0.19	0.01
	1.5	34.46	−0.01	−0.72	0.31	−3.54	−0.15	−0.27	0.04
	1.7	58.96	−0.51	−1.77	0.36	−2.19	−0.15	−0.39	0.04
	1.9	96.58	0.42	−3.63	−0.13	*0.33	−0.15	−0.56	−0.07
4	1.6	54.36	0.02	−0.88	0.31	−1.80	−0.16	−0.32	0.06
	1.8	87.36	−0.70	−2.19	0.33	*0.36	−0.16	−0.45	0.04
	2.0	135.7	−1.58	−4.34	−0.28	3.76	−0.24	−0.71	−0.01
	2.1	166.6	−2.32	−6.19	−0.59	6.08	−0.18	−0.82	−0.13
	2.2	181.9	−24.20	−29.45	19.86	7.48	−1.48	−2.30	1.06
6	2.0	160.4	−1.48	−3.47	0.07	6.78	−0.30	−0.63	0.05
	2.1	194.1	−2.04	−4.71	−0.39	9.42	−0.15	−0.63	−0.13
	2.2	233.6	−2.28	−5.95	−1.39	12.18	−0.30	−0.95	−0.03
	2.4	330.6	−4.06	−10.33	−3.53	19.44	−0.30	−1.32	−0.32
8	1.8	124.6	−0.72	−1.68	0.70	5.31	−0.05	−0.23	−0.12
	2.0	182.0	−1.44	−2.96	0.26	9.60	−0.11	−0.41	−0.11
	2.1	218.1	−1.81	−3.80	−0.33	12.16	−0.32	−0.68	0.01
	2.3	307.3	−3.29	−6.55	−1.95	18.80	−0.40	−1.03	−0.06
	2.5	389.3	−38.90	−44.68	29.19	24.56	−3.28	−4.28	2.52
	2.7	524.7	−53.32	−62.66	36.81	35.04	−3.60	−5.05	2.33
15	2.1	287.5	−1.35	−6.88	−0.13	20.55	−0.15	−0.90	−0.17
	2.4	451.5	−3.54	−4.15	−2.64	33.15	−0.30	−0.28	−0.40
	2.7	682.2	−7.52	—	−7.59	49.80	−0.90	—	−0.46
	3.0	995.5	−12.50	—	−16.49	71.70	−1.20	—	−1.00
Average errors/(%)			1.97	3.71	1.56		4.08	9.16	2.31

Note: (a) The parameters(α_2, α_3) in the generalized morse-potential used in the calculation are (5.93, 2.10) for $\alpha_1=13.5$. (b) Numbers in columns labeled as Δ_{mWCA}, Δ_{RHNC} and Δ_{XS} denote the respective deviations from the simulation results, $\Delta_{(\cdots)}=X_{simul}-X_{(\cdots)}$. The data points labeled '*' have not been included in the calculations of errors.

Table 4　Comparison of the results of reduced pressure(pr_e^3/ε_0) and reduced internal energy($U/N\varepsilon_0$) for the Exp-6 fluids with $\alpha=14.5$ calculated in this work(XS) with that of molecular dynamic simulations, mWCA and RHNC theories by Vortler et al.[13]

kT/ε_0	ρr_e^3	pr_e^3/ε_0				$U/N\varepsilon_0$			
		MD	Δ_{mWCA}	Δ_{RHNC}	Δ_{XS}	MD	Δ_{mWCA}	Δ_{RHNC}	Δ_{XS}
2	1.0	4.500	−0.04	−0.22	0.05	−4.10	−0.06	−0.07	−0.01
	1.2	9.920	0.01	−0.27	0.11	−4.66	−0.10	−0.13	0.02
	1.4	20.58	−0.03	−0.69	0.25	−4.76	−0.12	−0.24	0.07
	1.6	39.92	−0.21	−1.88	0.28	−4.00	−0.06	−0.33	0.01
	1.7	51.53	−3.16	−5.58	2.82	−3.60	−0.42	−0.79	0.33
3	1.1	11.39	−0.30	−0.19	0.06	−3.78	−0.09	−0.12	−0.01
	1.3	21.31	−0.06	−0.40	0.23	−3.87	−0.12	−0.20	0.05
	1.5	38.63	−0.07	−1.00	0.41	−3.27	−0.15	−0.28	0.07
	1.7	67.23	−0.45	−2.40	0.38	−1.71	−0.15	−0.46	0.08
	1.8	86.73	−1.34	−4.07	0.67	*−0.39	−0.11	−0.53	0.01
4	1.2	20.68	−0.06	−0.29	0.16	−3.16	−0.08	−0.14	−0.01
	1.4	36.05	−0.13	−0.62	0.39	−2.72	−0.16	−0.25	0.07
	1.6	61.14	−0.24	−1.38	0.51	−1.44	−0.24	−0.40	0.15
	1.7	78.56	−0.42	−2.12	0.53	*−0.16	−0.02	−0.29	−0.04
	1.8	100.2	−0.74	−3.03	0.31	1.08	−0.20	−0.58	0.12
6	1.6	78.5	−0.03	−1.09	0.47	*0.78	−0.18	−0.36	0.12
	1.7	98.39	−0.78	−1.72	0.59	2.34	0.03	−0.21	−0.09
	1.8	122.6	−0.74	−2.52	0.54	3.84	−0.18	−0.48	0.09
	2.0	186.0	−2.28	−5.57	0.46	8.52	−0.12	−0.64	−0.07
	2.2	276.4	−2.52	−8.99	−2.10	14.82	−0.30	−1.24	−0.07
8	1.7	114.2	−1.86	−3.09	2.16	4.32	−0.17	−0.37	0.07
	1.8	142.1	−0.75	−2.41	0.78	6.24	−0.16	−0.44	0.07
	2.0	209.2	−3.76	−6.32	2.14	11.36	−0.16	−0.58	−0.04
	2.2	305.8	−3.26	−8.34	−0.91	18.08	−0.40	−1.17	0.05
	2.4	434.2	−3.94	−13.10	−4.79	27.28	−0.40	−1.71	−0.21
15	1.7	167.0	0.48	−1.17	0.26	10.80	0.00	−0.18	−0.22
	2.0	283.7	−0.70	−3.96	−0.40	19.65	−0.15	−0.59	−0.13
	2.3	461.7	−3.36	−7.84	−2.15	32.85	−0.30	−1.07	−0.15
	2.6	721.6	−8.87	−29.52	−5.87	51.30	−0.90	−2.91	−0.25
	2.9	1091.0	−12.16	—	−17.34	76.35	−1.20	—	−0.85
Average errors/(%)			0.95	2.91	0.93		3.99	10.1	2.25

Note: (a) The parameters(α_2, α_3) in the generalized morse-potential used in the calculation are (6.21, 2.32) for $\alpha_1=14.5$.
(b) Numbers in columns labeled as Δ_{mWCA}, Δ_{RHNC} and Δ_{XS} denote the respective deviations from the simulation results, $\Delta_{(\cdots)}=X_{simul}-X_{(\cdots)}$. The data points labeled '*' have not been included in the calculations of errors.

Table 5 Average errors of reduced pressure and reduced internal energy calculated from the mWCA, RHNC and analytic Ross theories(XS) as compared with the MD simulation results of Vortler et al.[13] (%)

α	pr_e^3/ε_0			$U/N\varepsilon_0$		
	mWCA	RHNC	XS	mWCA	RHNC	XS
11.5	2.59	3.69	1.82	4.65	10.2	2.96
12.5	2.55	4.15	1.57	6.65	14.1	6.95
13.5	1.97	3.71	1.56	4.08	9.2	2.31
14.5	0.95	2.91	0.93	3.99	10.1	2.25
Average	2.02	3.62	1.47	4.84	10.9	3.62

Table 6 The value of parameters of α_1, α_2 and α_3

α_1	α_2	α_3	α_1	α_2	α_3	α_1	α_2	α_3	α_1	α_2	α_3
11.5	5.22	1.52	12.5	5.60	1.74	13.5	5.93	2.10	14.5	6.21	2.32

5 Application to Fluid N_2

We now apply the new EOS to N_2 fluid, The values of parameters obtained α_1, α_2, α_3, ε/k and r_e are 14.8, 6.267, 2.36, 97.6 K and 0.406 4 nm, respectively. As shown in Fig. 2, the calculated results are in a surprisedly good agreement with the experiment with only 0.9% deviation. With further intention to examine the application to a wider range of pressure and temperature, the foregoing parameters and the analytic expression are further employed to the range of pressure above 1 GPa for prediction. In Table 7, According to Strak et al.[20], numbers in columns labeled as "Ref. [20]" is believed superior to those obtained by using empirical Morse potential in Ref. [18], the agreement with them is very satisfactory with 1.35% deviation, which verifies the reasonability of this work and application to real fluids in a wide range of pressure and density.

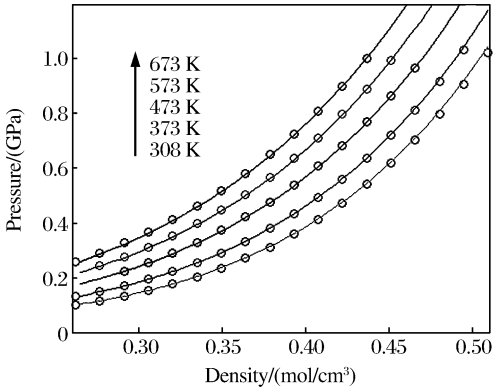


Fig. 2 Comparison of the results of pressure of nitrogen at integral density calculated in this work with those of Ref. [17]

Table 7 Comparison of the nitrogen pressures derived from Ref. [20] and this work

Density /(g/cm³)	T /(K)	Pressure/(GPa)			Density /(g/cm³)	T /(K)	Pressure/(GPa)		
		Ref. [21]	Ref. [20]	This work			Ref. [21]	Ref. [20]	This work
1.3	1011.0	2.81	3.97	3.95	1.3	2036.4	3.94	5.68	5.70
1.5	1000.6	4.61	6.70	6.65	1.5	2041.0	6.13	8.99	9.06
1.7	985.6	7.25	10.79	10.69	1.7	2042.0	9.18	13.69	13.88
1.9	985.6	10.87	16.77	16.58	1.9	2023.0	13.19	20.13	20.53
2.1	993.7	15.83	25.12	24.78	2.1	2033.0	18.44	28.89	29.60
2.3	1006.2	22.22	36.41	35.81	2.3	1976.4	25.18	40.06	41.20

6 Summary

We have shown that, by using the analytic PY expression of radial distribution function of hard spheres, it is possible to establish simple analytic EOS for the fluids with generalized Morse potential based on the Ross variational perturbation theory. The extensive comparison of the numerical results with the computer simulations has demonstrated the validity of the model and higher precision of the analytic Ross theory than that of mWCA and RHNC theory. Application to fluid N_2 shows that the new EOS is applicable to real fluid over wide range of temperature and pressure. It is practically meaningful to extend it to other real fluids such as H_2, O_2, CH_4, and CO_2, α of which vary within the range $\{13.34, 14.48\}$ and considered temperature 300 K$<T<$4 000 K according to Vortler et al.[13].

Appendix

$$G(t) = tL(t)/Q(t) \tag{A1}$$

$$Q(t) = 12\eta L(t) + S(t)\mathrm{e}^t \tag{A2}$$

$$Q'_\eta(t) = 12L(t) + 12\eta L'_\eta(t) + S'_\eta(t)\mathrm{e}^t \tag{A3}$$

$$Q'_t(t) = 12\eta L'_t(t) + S'_t(t)\mathrm{e}^t + S(t)\mathrm{e}^t \tag{A4}$$

$$Q''_{\eta t}(t) = 12L'_t(t) + 12\eta L''_{\eta t}(t) + S''_{\eta t}(t)\mathrm{e}^t + S'_\eta(t)\mathrm{e}^t \tag{A5}$$

$$Q''_{tt}(t) = S''_{tt}(t)\mathrm{e}^t + 2S'_t(t)\mathrm{e}^t + S(t)\mathrm{e}^t \tag{A6}$$

$$L(t) = (1+\eta/2)t + (1+2\eta) \tag{A7}$$

$$S(t) = (1-\eta)^2 t^3 + 6\eta(1-\eta)t^2 + 18\eta^2 t - 12\eta(1+2\eta) \tag{A8}$$

$$G'_\eta(t) = G(t)L^{-1}(t)L'_\eta(t) - G^2(t)[tL(t)]^{-1}Q'_\eta(t) \tag{A9}$$

$$G'_t(t) = G(t)[t^{-1} + L^{-1}(t)L'_t(t)] - G^2(t)[tL(t)]^{-1}Q'_t(t) \tag{A10}$$

$$\begin{aligned} G''_{\eta t}(t) = {} & G'_t(t)L^{-1}(t)L'_\eta(t) + G(t)L^{-2(t)}[L(t)L''_{\eta t}(t) - L'_\eta(t)L'_t(t)] - \\ & G^2(t)[tL(t)]^{-2}[2Q(t)G'_t(t) - L(t) - tL'_t(t)]Q'_\eta(t) - G^2(t)[tL(t)]^{-1}Q''_{\eta t}(t) \end{aligned} \tag{A11}$$

$$\begin{aligned} G''_{tt}(t) = {} & G'_t(t)[t^{-1} + L^{-1}(t)L'_t(t)] - G(t)[t^{-2} + L^{-2}(t)L'_t(t)L'_t(t)] - \\ & G^2(t)[tL(t)]^{-2}[2Q(t)G'_t(t) - L(t) - tL'_t(t)]Q'_t(t) - G^2(t)[tL(t)]^{-1}Q''_{tt}(t) \end{aligned} \tag{A12}$$

References:

[1] Barker J A, Henderson D. Perturbation Theory and Equation of State for Fluids (Ⅱ)—A Successful Theory of Liquids [J]. J Chem Phys, 1967, 47(11): 4714-4721.

[2] Weeks J D, Chandler D, Andersen H C. Role of Repulsive Forces in Determining the Equilibrium Structure of Simple Liquids [J]. J Chem Phys, 1971, 54(12): 5237-5247.

[3] Ross M. A High-Density Fluid-Perturbation Theory Based on an Inverse 12th-Power Hard-Sphere Reference System [J]. J Chem Phys, 1979, 71(4): 1567-1571.

[4] Ross M, Ree F H, Young D A. The Equation of State of Molecular Hydrogen at Very High Density [J]. J Chem Phys, 1983, 79(3): 1487-1494.

[5] Holmcs N C, Ross M, Ncllis W L. Temperature Measurements and Dissociation of Shock-Compressed Liquid Deuterium and Hydrogen [J]. J Phys Rev B, 1995, 52(22): 15835-15845.

[6] Tang Y. Role of the Barker-Henderson Diameter in Thermodynamics [J]. J Chem Phys, 2002, 116(15): 6694-6700.

[7] Tang Y, Lu B C-Y. An Analytical Analysis of the Square-Well Fluid Behaviors [J]. J Chem Phys, 1994, 100(9): 6665-6671.

[8] Tang Y, Wang Z, Lu B C-Y. Thermodynamic Calculations of Linear Chain Molecules Using a SAFT Model [J]. J Mol Phys, 2001, 99(1): 65-76.

[9] Kang H S, Lee C S, Ree T, et al. A Perturbation Theory of Classical Equilibrium Fluids [J]. J Chem Phys, 1985, 82(1): 414-423.

[10] Lado F. Perturbation Correction for the Free Energy and Structure of Simple Fluids [J]. J Phys Rev A,1973,8(5):2548-2552.

[11] Lado F,Foiles S M,Ashcroft N W. Solutions of the Reference-Hypernetted-Chain Equation with Minimized Free Energy [J]. J Phys Rev A,1983,28(4):2374-2379.

[12] Talbot J,Lebowitz J L,Waisman E M,et al. A Comparison of Perturbative Schemes and Integral Equation Theories with Computer Simulations for Fluids at High Pressures [J]. J Chem Phys,1986,85(4):2187-2192.

[13] Vortler H L,Nezbeda I,Martin L. The Exp-6 Potential Fluid at Very High Pressures:Computer Simulations and Theory [J]. J Mol Phys,1997,92(5):813-824.

[14] Wertheim M S. Exact Solution of the Percus-Yevick Integral Equation for Hard Spheres [J]. J Phys Rev Lett,1963,10(8):321-323.

[15] Thiele E. Effect of Pressure on the Resistance of Fused-Ring Aromatic Compounds [J]. J Chem Phys,1963,39(3):474-479.

[16] Michels A,Lunbeck R J,Wolker J. Thermodynamical Properties of Nitrogen as Functions of Density and Temperature between −125 ℃ and +150 ℃ and Densities up to 760 Amagat [J]. J Physica,1951,17(9):801-816.

[17] Robertson S L,Babb S E Jr. Isotherms of Nitrogen to 400 ℃ and 10000 ℃ [J]. J Chem Phys,1969,50(10):4560-4564.

[18] Johnson J D,Shaw M S,Holian B L. The Thermodynamics of Dense Fluid Nitrogen by Molecular Dynamics [J]. J Chem Phys,1984,80(3):1279-1294.

[19] Strak P,Krukowski S. Equation of State of Nitrogen(N_2) at High Pressures and High Temperatures:Molecular Dynamics Simulation [J]. J Chem Phys,2006,124(13):1345011-1345019.

[20] Strak P,Krukowski S. Molecular Nitrogen-N_2 Properties:The Intermolecular Potential and the Equation of State [J]. J Chem Phys,2007,126(19):1945011-1945018.

[21] Barin I. Thermochemical Data of Pure Substances(3rd ed) [M]. New York:Wein-Heim,1994:79-101.

[22] Carnahan N F,Starling K E. Equation of State for Nonattracting Rigid Spheres [J]. J Chem Phys,1969,51(2):635-636.

[23] Frisch H L,Katz J L,Praestgaard E,et al. High-Temperature Equation of State-Argon [J]. J Phy Chem,1966,70(6):2016-2020.

广义 Morse 流体解析状态方程及对氮的应用

薛新英,孙久勋,田荣刚

(电子科技大学应用物理系,四川成都 610054)

摘要:根据 Ross 变分微扰理论以及硬球流体 Percus-Yevick(PY) 径向分布函数表达式,建立了广义 Morse 势流体的解析状态方程。与模拟结果的比较一方面证实了广义 Morse 势模型的合理性;另一方面表明了解析 Ross 变分微扰理论的精度相当或略好于非解析的 Weeks-Chandler-Anderson(mWCA)理论,而优于复杂的优化超网络链积分方程理论(RHNC)。该解析状态方程被应用于拟合处于环境温度和压强小于 1 GPa 情形流体氮的实验数据,所得到的势能参数被用于预测高温高密度情形氮流体的压强,预测结果证实,该解析状态方程可以很好地适用于较宽的压强和温度范围。

关键词:状态方程;热力学量;解析性;变分

中图分类号:O521.2 **文献标识码**:A